A one-two punch: Joint effects of natural gas abundance and renewables on coal-fired power plants*

Harrison Fell† and Daniel T. Kaffine‡

November 12, 2014

Abstract

Since 2007, coal-fired electricity generation in the US has declined by a stunning 25%. At the same time, natural gas-fired generation and wind generation have dramatically increased due to technological advances and policy interventions. We examine the joint impact of natural gas prices and wind generation on coal generation, with a particular focus on the interaction between low natural gas prices and increased wind generation. Exploiting detailed daily unit-level data, we estimate the response of coal-fired generation across four transmission regions within the US. Low natural gas prices and increased wind generation have both led to reductions in coal-fired generation. Furthermore, we find evidence that the interaction between natural gas prices and wind generation is statistically and economically significant, and led to a greater reduction in coal-fired generation than would be explained by either factor alone. In some regions, marginal responses of coal-fired generation to natural gas prices in 2013 were several times what they would have been had wind generation remained at 2008 levels. Similar sensitivities were found for responses to wind generation. As a consequence, our results suggest that policies such as carbon pricing combined with those that increase wind generation would be complementary in terms of their impact on coal-fired generation.

*We thank Ventyx for providing access to their Velocity Suite database tool. Seminar and workshop participants at Colorado State, CU Boulder, the Front Range Energy Camp and the CU Environmental and Resource Economics Workshop provided valuable feedback.

†Division of Economics and Business, Colorado School of Mines; hfell@mines.edu

‡Department of Economics, University of Colorado Boulder; daniel.kaffine@colorado.edu

1 Introduction

The electricity generation profile of the U.S. has changed significantly over the last several years. Coal-fired generation, once representing a strong majority of U.S. electricity generation, has declined approximately 25% from 2007 to 2013, reducing associated annual carbon dioxide emissions from coal by a substantial 500 million tons of CO_2.[1] At the same time, a dramatic decrease in natural gas prices, largely due to an increase in supply brought about by hydraulic fracturing extraction techniques, has led to substantial increases in gas-fired generation (Joskow 2013). Renewable generation, particularly wind, has also increased dramatically, driven by state-level renewable portfolio standards (RPS), federal production and investment tax credits, and technological advances (Schmalensee 2012). Clearly, these changes in coal, gas and wind generation are related, but how? In terms of the impact on coal-fired generation, are wind and gas complements or substitutes? Do these impacts vary across regions? Will policies that promote renewable development increase or decrease the effectiveness of carbon pricing? In this paper, we empirically examine how decreased natural gas prices and increased wind generation have individually and jointly affected coal-fired generation and emissions, in order to understand the effectiveness of future overlapping energy and environmental policies.

The focus on the electricity generation sector is motivated by several important factors. First, the electricity generation sector is an important anthropogenic source of local and global pollutants, such that even small changes in this sector may have profound impacts on air quality and total climate-related emissions. This is shown in Figure 1, which displays the

[1] At current estimates of the social cost of carbon, this represents approximately $20 billion dollars in avoided social damages annually from CO_2 alone.

substantial CO_2 emissions from the electricity sector relative to other sectors over the last decade. Second, the last decade has witnessed substantial change within the electricity generation sector, per Figure 2, which illustrates the growth of wind and natural gas generation and the decline of coal generation. Importantly, while Figure 1 shows that the decline in CO2 levels from 2005 to the present is mainly attributable to the electricity sector, Figure 2 shows that demand has played very little role.[2] Instead, the shift out of coal towards wind and gas looks to be driving a large fraction of the decline in US CO_2 emissions.[3]

While these figures provide some insight into the evolving electricity sector, the interaction between wind, gas and coal is a complex relationship based on generation costs, demand levels, and intermittency issues (Joskow 2011; Godby et al. 2013). Understanding these relationships is a pressing need, as policies such as renewable portfolio standards and potential carbon pricing, interacting with market factors such as fracking and natural gas export, suggest that the electricity sector will continue to evolve in dramatic ways over the next several decades. Given that coal accounts for roughly 25% of US CO_2 emissions, it is not an overstatement to say that understanding the future evolution of coal-fired generation is the key and crucial aspect in terms of US sources of carbon emissions and impact on global climate change.

Our paper contributes to a growing literature examining the impacts of renewables and

[2] A decline in demand for electricity due to recessionary impacts would be a plausible explanation for the decline in emissions from the electricity sector; however, total electricity demand is essentially flat from 2005 (4,055,423 GWh) to the present (4,058,209 GWh). This flat national trend does hide some variation in regional trends, for example total electricity demand is down 14% in New England and up 10% in West South Central (TX, OK, AR, LA). One might be concerned that shifts in regional generation could affect emissions due to regional variations in generation mix, however our regional analysis accounts for changes in regional demand.

[3] Total CO_2 emissions declined by 729 million tons from 2005 to 2012, with the decrease in emissions from the electricity sector accounting for more than half of that decline. Of course, to the extent that gas is displacing coal, increases in gas generation produce their own CO_2 emissions, but at a much lower rate than coal leading to net emission savings from coal-to-gas switching (Lafrancois 2012).

low natural gas prices on the electricity generation sector. Many of these studies use simulated dispatch models over varying time horizons to determine both generation and capacity expansion possibilities in a variety of policy and market contexts.[4] As an alternative to simulating behavior, several studies have turned to observed data to determine how policies and changing market conditions affect existing generators. For example, Novan (2013), Cullen (2013) and Kaffine et al. (2013) use data from the Electricity Reliability Council of Texas (ERCOT) to determine emissions offset by wind generation, which also provides insight into which generation technologies are being displaced.[5] These papers generally find increased wind generation primarily displaces natural-gas-fired generation. However, many of these studies cover time periods (mid-to-late 2000s) when natural gas prices were relatively high and wind constituted a small portion of the generation mix.

Recently, several studies have also examined the effect of low US natural gas prices on generation profiles and emissions.[6] These papers have generally found evidence of a shift in generation towards natural gas as prices have fallen, suggesting natural gas generators have become inframarginal, pushing coal generators to become marginal generators. For instance, Holladay and LaRiviere (2014) and Linn et al. (2014) find some evidence that in certain NERC regions, low natural gas prices have significantly altered marginal emission

[4] For example, several recent simulated dispatch studies predict generation and capacity investments under different energy and environmental policy scenarios. See for example, Holttinen and Tuhkanen (2004) Denholm et al. (2005), Newcomer et al. (2008), Katzenstein and Apt (2009), Traber and Kemfert (2011), Fell and Linn (2013), Bushnell et al. (2014). While these types of studies provide substantial valuable information, the models generating these results have many imposed assumptions about generator responses and transmission possibilities, among other issues. Such assumptions may lead to a considerable wedge between expected and observed outcomes.

[5] See also Callaway and Fowlie (2009) and Amor et al. (2014) for similar studies of wind in the US Northeast and Ontario.

[6] Older papers examining fuel substitution behavior include Atkinson and Halvorsen (1976), Griffin (1977), Joskow and Mishkin (1977), and Bopp and Costello (1990). More recently, Pettersson et al. (2012) examine fuel substitution in Western Europe.

rates. Similarly, using regionally aggregated emissions data, Cullen and Mansur (2013) and Lu et al. (2012) have found empirical evidence of CO_2 emissions reductions in the electricity generation sector in response to recently lower natural gas prices. Similarly, Soloway (2013) examines hourly and daily unit-level decisions by oil-gas switching plants in New York City from 2005-2010 and Linn et al. (2014) examine annual unit-level decisions by coal-fired plants in response to changes in fuel input prices from 1985-2009. To our knowledge, however, no prior studies have jointly considered the effect of falling natural gas prices and increased renewable generation.

Relative to existing econometric models in this area, our approach will expand the literature in several key ways. First, we will conduct our analysis across several Independent Systems Operator (ISO) regions, as opposed to regionally specific models.[7] This allows us to examine varying affects by region, due to varying generation capacities, transmission possibilities, and regulatory regimes, giving us a much more comprehensive view of generator responses. Second, rather than regionally aggregated data, we use daily generation-unit level data, which allows us to exploit more variation in input and output prices, load conditions, and wind generation.[8] Finally, and most importantly, our analysis will jointly analyze the effects of renewable generation, relative fuel prices, and interactions between these components. This allows for a more comprehensive analysis of the two most drastically changing features, renewable generation and abundant natural gas, of the electricity generation sector.

[7] Technically, some of the transmission regions we consider are Regional Transmission Organizations (RTO), which have similar but slightly more expansive responsibilities than ISO's. We refer to both ISO's and RTO's as simply ISO's in this study.

[8] The use of daily generation-unit data does pose some challenges due to the substantial number of days when when generating units do not run. We address those below with a) a censored-quantile regression approach as recently proposed by Galvao et al. (2013), and b) a traditional Heckman two-step estimation approach (Heckman 1979).

Analysis of the response of electricity generators to either of these factors in isolation may be missing important interaction effects. For example, a low natural gas price regime may lead to more coal on the margin, implying more coal would be offset by increased wind generation than if natural gas prices were high and gas was more likely on the margin. Alternatively, the fact that gas turbines are better suited than coal for ramping in response to the intermittency of wind may mean that more gas is dispatched to handle the volatility associated with higher levels of wind generation. How gas prices and renewables interact to affect daily operating decisions (the "operating margin") is a key focus of this study.[9]

Our paper also contributes to the literature on overlapping policies. While the previous literature has frequently focused on assessing the efficiency of single policy instruments (e.g. Fischer and Newell (2008) examine carbon policies as well as a portfolio of polices to address multiple market failures), there is growing recognition that multiple policies may overlap and interact in important ways.[10] Recent papers such as Goulder and Stavins (2011) and Goulder et al. (2012), have noted the potential for more stringent, quantity-based state policies to generate leakage at the federal level, reducing their effectiveness.[11] However, it is also possible that overlapping policies may have important impacts at the production level that crowd out or enhance the effectiveness of each policy. For example, using a structural model of automobile markets, Roth (2014) considers overlapping policy interactions between

[9] Of course, low natural gas prices and increased wind generation may also impact the longer-run "build margin" or retirement decisions of coal plants. We view this as an obvious area for future research.

[10] Policies relevant to the electricity sector may overlap at varying scales. For example, state-state: California's AB 32 carbon cap and trade program and California's RPS, federal-state: national carbon pricing and the more than 30 states with an RPS, or federal-federal: national carbon pricing and production tax credits (PTC) for renewables.

[11] Intuitively, by meeting the more stringent state policy, "slack" is created in the federal policy. In general, the literature has focused on the problems created by overlapping policies when one of the policies is quantity-based (Böhringer et al. 2008; Böhringer and Rosendahl 2010; Fischer and Preonas 2010; Levinson 2010).

a fuel-efficient vehicle tax credit and either a feebate or miles-per-gallon standard - a feebate enhances the effects of the tax credit, while the standard undermines it. Similarly, using our econometric estimates, we are able to generate a simple policy simulation analysis to examine whether or not overlapping policies related to electricity production, (e.g a carbon tax and a production tax credit for renewables), are complements or substitutes.

We find that low natural gas prices and increased wind generation have both led to reductions in coal-fired generation and CO_2 emissions from coal-fired plants. Furthermore, we find evidence that the interaction between natural gas prices and wind generation is statistically and economically significant in most regions. Indeed the interaction effect is large enough such that in some regions, the marginal response of coal-fired generation to natural gas price changes in 2013 were several times larger than they would have been had wind generation remained at 2008 levels. Likewise, some regions also experienced marginal responses of coal-fired generation to wind generation that was multiple times larger than it would have been had natural gas prices remained at relatively high 2008 levels. We also show that the existence of this interaction effect implies that policies such as carbon pricing combined those that increase wind generation would be complementary in terms of their impact on reducing coal-fired generation and emissions.

2 Background on electricity markets and dispatch curves

In this section, we provide some background on electricity markets, describe the pre-2008 view of the short-run supply curve, and motivate how the post-2008 fall in gas prices and increase in wind generation may have complementary effects in terms of reducing coal-fired

generation. The supply side of electricity markets is characterized by different generators with different fuel types and technologies, each with their own fixed capacities and marginal costs of generation. As a result, ordering generators by marginal cost, the short-run supply or "dispatch" curve is a step-function characterized by discrete jumps in marginal cost. For any given level of demand in a competitive market, the lowest marginal cost generators are dispatched until the market clears, with the wholesale price of electricity determined by the marginal cost of the final marginal generator. Those generators with marginal costs below the market-clearing marginal generator are thus inframarginal, while generators with higher marginal costs will simply not run. For the inframarginal generators, the capacity factor (actual generation divided by potential generation) will be near 1, while the marginal generator will typically operate at a capacity factor below 1.

Consider a simplified dispatch model where the supply side consists of four generators, two coal and two gas. The coal generators are differentiated by their marginal cost, where the low-cost generator has marginal cost of C_L and the high-cost generator has a marginal cost of C_H, and similarly for gas - G_L and G_H. Each generator is assumed to have the same capacity K. For simplicity, assume a constant level of demand D, equal to $3.5K$. Figure 3 Panel A illustrates this basic set-up. The dashed-grey lines represent the pre-2008 state of the world, where the highest-cost coal plant had lower marginal costs than the cheapest gas plant ($C_L < C_H < G_L < G_H$). Given demand D, both coal plants are fully dispatched (capacity factor of 1). By contrast only the low-cost gas plant is fully dispatched, with the high-cost gas plant operating at a capacity factor of 0.5. This set-up matches the typical textbook discussion of electricity markets where coal plants supply low-cost "baseload," with higher-cost gas plants used to meet "peak" demand.

However, as noted in the introduction, post-2008 has witnessed a dramatic drop in natural gas prices and a large increase in zero marginal cost wind generation. Panel A illustrates the effect of the fall in natural gas price. While the low-cost natural gas plants G_L swap position with the high-cost coal plants C_H in the dispatch curve, high-cost gas G_H remains the marginal generator, leading to no reduction in coal-fired generation.[12] Panel B illustrates the effect of an increase in wind generation W. The marginal generator switches from high-cost gas G_H to low-cost gas G_L, but the same amount of coal-fired generation is produced.[13]

Panel A and Panel B considered the effect of a change in gas price and wind generation individually, with no resulting change in coal-fired generation. In Panel C, gas price and wind generation changes are considered jointly. Considering first the drop in gas price, we have the reordering of the dispatch curve (C_H and G_L swap) per Panel A, followed by the increase in wind generation W. Now the marginal generator is high-cost coal C_L which runs at half capacity, reducing the overall coal capacity factor from 1 to 0.75. Alternatively, one can first think of the increase in wind production W leading to G_L as the marginal generator per Panel B, followed by a drop in natural gas prices, which swaps G_L with C_H. Again, the marginal generator would be high-cost coal C_H and coal capacity factor would drop.

While simplified, the above example illustrates that natural gas and wind may have complementary effects in terms of off-setting coal generation due to changes in the dispatch order. Furthermore, natural gas plants are generally better suited for ramping and quick adjustments to generation, while coal is designed for steady levels of constant generation. This may provide another channel by which increases in intermittent wind generation are

[12] This is consistent with the findings in Cullen and Mansur (2013) whereby a small increase in the price of CO_2 would induce little coal-to-gas switching if future relative fuel prices were similar to historic levels.

[13] This is consistent with the results in Novan (2013), Cullen (2013) and Kaffine et al. (2013), whereby only small amounts of coal are offset by wind generation in Texas in the mid-late 2000s.

paired with increased gas generation to handle the volatility of wind, at the expense of less-flexible coal generation.[14] Of course, the real electricity sector is far more complicated than the simple example presented above, and thus we turn to the data to examine the existence of any interaction effect and quantify its magnitude.

3 Data and methods

3.1 Data

As mentioned above, our analysis employs daily, unit-level data. All data sources we employ were made available to us by the energy data service company Ventyx via their Velocity Suite data management product, which organizes all publicly available datasets on electricity generating facilities in a single searchable database. We begin by creating daily capacity factors and emissions for coal-fired generating units. The daily capacity factor measure, CF_{it}, is calculated as unit i's net generation (generation produced less power needed to operate the unit) on day t divided by its daily generating capacity, $CF_{it} = \frac{NetGen_{it}}{GenCapacity_i}$. To determine the $NetGen_{it}$ for a given unit, we create daily aggregates of hourly net generation (megawatt hour - MWh) based on EPA's Continuous Emissions Monitoring System database(CEMS).[15] The daily generation capacity is based on the given nameplate capacity (megawatt - MW) for

[14] It would stand to reason that if load-balancing entities would prefer to have more flexible natural gas-fired generation running to support intermittent wind generation that they would be more likely to employ even more gas generation on the system for intermittency-support reasons if the price of natural gas generation decreases. This behavior would lead to wind generation and natural gas price interaction effects on coal-fired generation.

[15] Because plant operators report gross generation (total generation of electricity at a plant) to CEMS, Ventyx estimates net generation in their database. Ventyx first calculates the ratio of net generation to gross generation using data from the NERC Generating Availability Data System (GADS). Then they multiply gross generation by this ratio to calculate net generation.

each unit in the sample, where $GenCapacity_i = (nameplate\,capacity)_i \times 24$. The nameplate capacity for the generation units comes from the EIA's 860 form.

The CEMS database also includes hourly CO_2 emissions by unit and we use this to create our emissions variable.[16] The CO_2 emission variable we create is similarly a capacity-weighted measure. More specifically, our emissions dependent variable, E_{it} is calculated as $E_{it} = \frac{(emission\,of\,CO_2)_{it}}{(nameplate\,capacity)_i}$, where emissions of CO_2 is measured in tons/day. We use a capacity weighted emissions measure to directly remove the variation in emissions due to the size of the generating unit and to make parameters more interpretable across heterogeneously sized coal-fired units. Also, while net generation and CO_2 emissions are positively correlated, they are not perfectly correlated. For example, coal-fired units often need to be warmed up after a complete shutdown, and can thus create positive emissions without positive net generation. This lack of perfect correlation between emissions and net generation motivates looking at the impacts of wind generation and relative natural gas price on both capacity factors and CO_2 emissions per unit of capacity.

The variables CF_{it} and E_{it} are formed for coal-fired units across the transmission regions of ERCOT, Midwestern Independent System Operator (MISO), PJM Interconnection (PJM), and Southwest Power Pool (SPP). These regions are displayed in Figure 4. These ISO's were selected because they have publicly available data for daily wind generation, have significant coal generation, and capture nearly two-thirds of wind generation in the United States.[17] Daily wind generation data was collected for each region over the period 2008

[16] Units subject to CEMS requirements are mandated to report continuous hourly emissions based on either a) direct gas measurements or b) continuous fuel feed monitoring and mass balance calculations. While not required to report emissions, units below 25 MW capacity do participate in power generation markets, though as noted in Kaffine et al. (2013) and Linn et al. (2014), these excluded generators are only a small percentage of the total market.

[17] Two other regions with significant wind generation are California ISO (CAISO) and Bonneville Power

- 2013 and used to form W_t, which identifies the wind generation in hundreds of gigawatt hours (GWh) in the ISO of interest on day t.[18]

The other key variable created for each unit is a coal-to-natural gas price ratio, $P_{it}^R = \frac{P_{it}^C}{P_{it}^G}$, which is used to measure the relative effect of changes in natural gas prices. The coal price, P_{it}^C, is a Ventyx-modeled monthly measure of the \$/MMBtu cost of coal for unit i.[19] P_{it}^C is therefore constant for all days t within a given month-year. This, however, is not a major limiting factor of the data as coal is typically contracted over relatively long periods and is therefore not volatile on a daily basis. The natural gas price P_{it}^G is modeled as the daily natural gas price, in \$/MMBtu, at the gas hub nearest to unit i, based on spot prices quoted by the Intercontinental Exchange (ICE). This gives us a good measure of the price at competing natural gas plants in the vicinity of coal unit i. In addition, there is considerable heterogeneity in gas prices across hubs, thus P_{it}^G, and subsequently P_{it}^R, has considerable variation both temporally and cross-sectionally allowing for stronger identification.

We also gathered several other key explanatory variables. To control for regional power demand, referred to as "load", we collect the variable $Load_{it}$ which measures the power demanded in unit i's "transmission zone" area on day t.[20] Similarly, we collect the wholesale

Authority (BPA). However each of these regions only has a single coal plant, and thus fall outside the scope of our research question. Additionally, we also analyzed data from ISO-New England (ISONE) and New York ISO (NYISO). However, due to the combination of relatively low wind generation, few operating coal power plants, and the implementation of the Regional Greenhouse Gas Initiative (RGGI) in this region during the time span analyzed, we opted to omit these results from our analysis.

[18] One possible concern of using ISO as the geographic region for our estimations is that ISOs import and export power out of their territory. However, because we are focused on coal-fired generation which is typically baseload, we are less concerned about changes in imports/exports of coal-fired electricity due to daily changes in wind generation or natural gas prices within an ISO. To the extent there is some response in imports/exports of coal-fired electricity, our results below would be slight underestimates of the effect of natural gas prices and wind generation on coal-fired generation and emissions.

[19] Ventyx creates this coal price variable by using running averages of publicly available delivered coal prices given in EIA 923 forms. For plants not reporting these coal costs, Ventyx creates a price as a weighted average of surrounding plants.

[20] Transmission zones are Ventyx-created areas that, as stated in their documentation, "represent load pockets and these load pockets are derived through extensive analysis of FERC 714 data, ISO reports in

electricity price in unit i's transmission zone on day t, $pricemwh_{it}$. The variable age_{it} gives unit i's age in years as of day t. We also collect data on a unit's operating status, which signify if the unit is "operating", "mothballed", "standby", or "out of service." Our analysis only includes units designated as "operating." Many other variables were also collected on the units' regulatory status, emission control equipment, and environmental regulation program enrollments, but these variables are relatively constant over the sample we explore and thus dropped in most of our fixed effects estimation procedures.

The variables CF_{it}, E_{it}, P_{it}^{R}, W_{it}, and $Load_{it}$ are summarized by ISO in Table 1. In this table, the variable's mean and standard deviation are summarized over the entire sample under the columns "Mean" and "SD", respectively. The 2008 and 2013 mean values are also presented under columns "Mean-2008" and "Mean-2013, respectively. As can be seen in the table, average coal capacity factors and CO_2 emissions per unit of capacity have fallen from 2008 to 2013. At the same time, wind generation and the coal-to-natural gas price ratio have risen when comparing 2008 averages to those in 2013. This is due to expanding wind capacity and falling natural gas prices, respectively. Finally, despite the major changes to the supply side of the electricity sector, mean load values have remained relatively constant over 2008 to 2013. However, because we use daily data, there is still considerable variation in $Load_{it}$ in our sample.

ERCOT, WECC transmission cases and Multiregional Modeling Working Groups (MMWGs) in the Eastern interconnect." Load for these areas is reported via data provided by the ISO's.

3.2 Empirical strategy

The primary difficulty in estimating the impacts of natural gas prices and wind generation on coal-fired units' daily capacity factors and emissions is that coal plants, for various reasons, do not generate power every day. Thus, while daily data allows us to exploit considerable variation in wind generation and natural gas prices, daily data also results in many "0" observations for the dependent variables of capacity factor and CO_2 emissions. A second difficulty that arises in this context is that one may not expect the response to natural gas prices and wind generation to be constant over all groups of coal-fired generators. This is demonstrated to some degree in the simple dispatch model presented above. As natural gas prices drop and wind generation expands, some, but not necessarily all, coal generators will be pushed off the margin or at least forced to run at considerably reduced capacity factors. We would expect that the coal plants with lower marginal costs of production may remain inframarginal and therefore would appear less responsive to changes in natural gas prices and wind generation, while those with high marginal costs are the first to be pushed off the margin on days with high wind generation and/or low natural gas prices.

We deal with these issues through the use of two different estimation techniques. To begin with, given the censored dependent variables and the possibility for different responses over different groups of generators, we apply a censored-quantile regression approach, adapted to panel data models with fixed effects as recently proposed by Galvao et al. (2013). As shown in Galvao et al. (2013), the data censoring leads to a standard quantile regression objective function maximized over a subset of the data. The subset is defined as those observations where the conditional propensity score associated with being above the censoring point (i.e.

the propensity score of having a non-zero CF_{it} or E_{it}) is greater than $(1-\tau)$, where τ is the quantile value of interest. The Galvao et al. (2013) method therefore calls for a multi-step procedure in which one first estimates estimates the propensity score π_{it} and in the second step a standard quantile regression is run on the subset of observations that have $\pi_{it} > (1-\tau) + c_N$ where c_N is a user-specified small positive constant that approaches zero as N goes to infinity.[21]

To obtain the propensity score for this application we estimate a panel probit model using the method of Fernández-Val (2009), which allows for fixed effects.[22] The censoring occurs at zero for CF_{it} and E_{it}, so where the generating unit has no positive net generation or no emissions.[23] Defining z^*_{it} as the latent variable that, when greater than zero, leads unit i on day t to have a positive capacity factor or positive emissions, then the latent regression representation of this discrete-choice model is:

$$\begin{aligned} z^*_{it} = \gamma_1 P^R_{it} + \gamma_2 \left(P^R_{it}\right)^2 + \gamma_3 \left(P^R_{it}\right)^3 + \gamma_4 W_t + \gamma_5 W_t^2 + \gamma_6 W_t^3 + \gamma_7 \left(W_t * P^R_{it}\right) \\ + \gamma_8 D^S_{it} + \mathbf{x'_{it}}\boldsymbol{\phi} + \alpha_i + \eta_{sy} + u_{it} \end{aligned} \tag{1}$$

$$z_{it} = \begin{cases} 1 \text{ if } z^*_{it} \geq 0 \\ \\ 0 \text{ if } z^*_{it} < 0 \end{cases}$$

[21] For all results shown below we set $c_N = 0.05$, as was done in the application of Galvao et al. (2013). We tried other specifications of c_N and the results were similar to those shown here.

[22] The method of Galvao et al. (2013) allows for the formation of the propensity score through the estimation of non-parmetric or an alternative parametric discrete-choice method. We adopted the probit estimation here because we found that panel logit models in this application failed or took an extremely long time to converge, and because it was easier to implement than non-parametric discrete-choice models that account for the panel nature of the data.

[23] Note, as mentioned above, coal-fired units generally must be warmed up for some period before they begin generating power in instances where they are re-starting from a complete shutdown. This warming up period does lead to measurable emissions in the CEMS data set. Therefore, it is possible that a day may register positive CO_2 emissions, but not positive net generation and therefore a zero capacity factor. As such, it is necessary to run the selection step regression for capacity factor and CO_2 emissions separately.

We model this decision to run the unit as a flexible function of the the ratio of coal prices to natural gas prices P_{it}^R, ISO-level wind generation W_t, and the interaction of these two variables $\left(W_t * P_{it}^R\right)$.[24] To account for longer shutdown periods due to scheduled or unplanned maintenance, we include the dummy variable D_{it}^S, where $D_{it}^S = 1$ if day t is in a series of five or more consecutive days that unit i has $z_{it} = 0$. The point of this dummy variable is to correct for longer shutdown periods that appear to not be driven by contemporaneous market or renewable generation conditions.[25] The variable $\mathbf{x}_{it}$ controls for other relevant variables such as local load or wholesale electricity prices, unit age, and market regulatory status (i.e. if the unit is designated as "regulated" or "deregulated"). Unit-level fixed effects are captured in α_i and year-by-season fixed effects are accounted for in η_{sy}.[26] Thus identification is based from within season-year cross-sectional variation and from temporally within-unit variation. Finally, u_{it} represents the mean-zero disturbance term.

Given the estimated parameters of Equation (1), an estimated propensity score, $\hat{\pi}_{it}$, can be derived for each observation. We then find the parameters of the τ^{th} quantile regression

[24] We exclude higher polynomial terms of the interaction variable because much of the flexible response to wind and prices is picked up in the higher order W_t and P_{it}^R terms included. We also found that higher order interaction terms were highly correlated with one another, presenting a possible multi-collinearity issue.

[25] As noted in Kubik et al. (2012), plant maintenances are generally scheduled in advance and may last weeks. We have also explored different definitions for D_{it}^S by looking at a minimum of a seven day shutdown window. Results from these specifications are not materially different than those given here.

[26] In the actual estimation, unit fixed effects are estimated using unit-specific dummy variables. For the year-by-season effects, seasons are defined as winter if t is in months December through February; spring if t is in months March through May; summer if t is in months June through August; and fall if t is in months September through November.

as those that minimize:

$$Q\left(\boldsymbol{\beta}, \boldsymbol{\psi}, \boldsymbol{\kappa}, \boldsymbol{\omega}, \hat{\pi}\right) = \frac{1}{N\bar{T}} \sum_{i=1}^{N} \sum_{t=1}^{T_i} \rho_\tau \big[y_{it} - \beta_{1\tau} P_{it}^R + \beta_{2\tau} \left(P_{it}^R\right)^2 + \beta_{3\tau} \left(P_{it}^R\right)^3 + \beta_{4\tau} W_t + \beta_{5\tau} W_t^2 + \beta_{6\tau} W_t^3 + \beta_{7\tau} \left(W_t * P_{it}^R\right) + \mathbf{x_{it}'} \boldsymbol{\psi}_\tau + \kappa_{i\tau} + \omega_{sy\tau} \big] 1(\hat{\pi}_{it} > 1 - \tau + c_N) \tag{2}$$

In this specification, N is the number of cross-sectional units, $\bar{T}$ is the average number of observations per unit, T_i is the number of observations for unit i, $\rho_\tau(\cdot)$ is the standard loss function used in quantile regressions, y_{it} is the level of capacity factor or capacity-weighted emissions, κ_i are the unit-level fixed effects, ω_{sy} is the season-by-year fixed effect, and $1(\hat{\pi}_{it} > 1 - \tau + c_N)$ is an indicator function equal to one if $\hat{\pi}_{it} > 1 - \tau + c_N$ and zero otherwise. The indicator function therefore serves as the subset selector.[27] Note that this subset selection procedure does allow for some observations at the zero censoring level to be included in the regression.

The quantile regression technique allows us to have varying responses across quantiles, while still accounting for the censored nature of the data. The technique also allows us to simply calculate marginal effects, and importantly, counterfactual marginal responses, where we can view the marginal response to the price ratio assuming various levels of wind generation and vice versa. However, the data censoring in this application may be more appropriately framed in a "corner solution model" context (see Wooldridge (2002)). In this case, a Heckman two-step estimation (Heckman 1979) approach may be more consistent with the data generating process.

We therefore apply a Heckman two-step estimation approach, adapted to accommodate

[27] Galvao et al. (2013) also propose a three-step method that further refines the subset selection procedure. However, given the sizeable T in this application, their subset refinement step did not lead to a different subset selection than the two-step method presented here.

fixed effects in "large T" panel data sets, such as employed here, using the method described in Fernández-Val and Vella (2011). The method of Fernández-Val and Vella (2011) still has the traditional selection step estimation and intensity step estimation. The selection step estimation used here is the same panel probit model described in Equation (1) that models the unit's binary decision to have positive net generation or positive emissions. To estimate the second-step intensity equation, which models the determinants of the level of capacity factor or emissions conditional on the unit having positive net generation or emissions, we first need to recover the inverse Mills ratio, λ_{it}, from the selection step. This, again, is done using the bias correction model described in Fernández-Val and Vella (2011). Given this, we estimate the following intensity equation for observations with $y_{it} > 0$ (i.e., observations with positive capacity factors or positive emissions):

$$\begin{aligned} y_{it} = \beta_1 P_{it}^R + \beta_2 \left(P_{it}^R\right)^2 + \beta_3 \left(P_{it}^R\right)^3 + \beta_4 W_t + \beta_5 W_t^2 + \beta_6 W_t^3 + \beta_7 \left(W_t * P_{it}^R\right) \\ + \theta \lambda_{it} + \mathbf{x_{it}'} \boldsymbol{\psi} + \kappa_i + \omega_{sy} + \epsilon_{it} \end{aligned} \tag{3}$$

where the coefficient vectors of $\boldsymbol{\psi}, \boldsymbol{\kappa}$, and $\boldsymbol{\omega}$ have the same interpretation as in Equation (2), but will not have the same estimated values, and ϵ_{it} is the mean-zero disturbance term. Note also that this formulation of the selection equation and intensity equation allows for the selection step to be partially determined by a variable that is excluded from the intensity equation, namely D_{it}^S. This exclusion restriction aids in the identification of the parameters in the intensity equation.

Again, the advantage of this two-step technique is that it is more consistent with the data generating process. It also allows us to estimate a marginal effect of the price ratio or wind generation that accounts for the response in both the selection decision and intensity decision. However, as presented in more detail below, the formation of the counterfactual

marginal effects inclusive of both the selection and intensity responses is not possible in this framework.

4 Results

In this section, we report the estimates from the regression models described above. We estimate both the quantile regression model and the two-step Heckman-style model for each ISO separately. We run separate estimations for each ISO for two reasons. First, given the different generation mixes and wind resource availability across ISO's, it would seem reasonable that capacity factors and emissions would have different responses to the price ratio and wind generation across ISO's. Second, from a more practical standpoint, the size of the data set with all ISO regions combined presented significant computational difficulties for both estimation procedures. Indeed, even running the estimation techniques separately for each ISO proved to be computationally burdensome in the larger regions.

4.1 Quantile Regression Approach

Estimation results for the ISO-specific median quantile regression results (estimates of Equation (2) with $\tau = 0.50$) using CF_{it} and E_{it} as dependent variables are given in Tables 2 and 3, respectively. Given the cubic form of Equation (2), the marginal effects of relative fuel prices P^R or wind generation W are not readily apparent from these tables, however, many of the parameters are statistically significant. Importantly, we find that the parameter on the price-wind interaction term $W * P^R$ is negative, implying a complementary relationship between low natural gas prices and high wind generation in terms of reducing coal-fired

generators' capacity factors and CO_2 emissions. This interaction is also statistically significant, at least at the ten percent level, across both dependent variable specifications and in all regions except MISO. The lack of significance in MISO is likely due to the generation capacity mix in that region. More specifically, looking at the ratio of combined cycle natural gas capacity (the lowest-cost natural gas-fired technology) to coal-fired generation capacity, we find that MISO has the lowest ratio of the four regions at about 0.35, which may limit its ability to switch out of coal-fired generation.[28] In addition, MISO has historically had a very high share of generation from coal-fired units (nearly 80%) relative to other regions, with very little generation coming from gas-fired units. This suggests that coal plants in MISO may be relatively more efficient compared to the natural gas units in that region.

The form of Equation (2) implies that the marginal effects of the coal-to-natural gas price ratio and wind generation are given by:

$$\frac{\partial y_{it}}{\partial P_{it}^R} = \beta_{1\tau} + 2\beta_{2\tau} P_{it}^R + 3\beta_{3\tau} \left(P_{it}^R\right)^2 + \beta_{7\tau} W_t \tag{4}$$

$$\frac{\partial y_{it}}{\partial W_t} = \beta_{4\tau} + 2\beta_{5\tau} W_t + 3\beta_{6\tau} W_t^2 + \beta_{7\tau} P_{it}^R \tag{5}$$

Given this form, we have calculated "actual" and "counterfactual" marginal effects of coal-to-natural gas price ratio and wind generation. The marginal effects for the capacity factor specifications are given in Table 4 and for the emissions specifications in Table 5. In these tables, we present the Actual marginal effects of P^R and W for 2008 and 2013. These Actual marginal effects are based on using the given year's (2008 or 2013) average values of P^R and W in the marginal effects equations (4) and (5) (i.e., we replace P_{it}^R and W_t values in (4) and (5) with their ISO-specific 2008 or 2013 average value counterparts). The

[28] By comparison, this ratio is roughly 0.4, 0.45, and 1.9 for PJM, SPP, and ERCOT, respectively.

"counterfactual" responses are given in the W2008 and P2008 columns. Under the W2008 column we calculate the given marginal effect assuming that wind generation remains at its 2008 level and, likewise, results in the P2008 column are calculated with P^R remaining at its 2008 average value. Thus, the 2013 rows give us a measure of what the marginal effects of P^R and W were with everything at their 2013 averages, as well as measure of what the marginal effects would have been had P^R or W remained at their relatively low 2008 levels.

The results presented in Table 4, display several readily apparent features. First, most of the marginal effects, and particularly those based on 2013-average variable values, are statistically significant.[29] Second, in most regions, the marginal effects of P^R and of W become more negative from 2008 to 2013. In part, this reflects the fact that across the ISO's, the marginal effect of P^R on CF becomes more negative as the coal-to-natural gas price ratio increases from 2008 to 2013 levels. This is consistent with Cullen and Mansur (2013) who show that decreasing the relative price of natural gas (via a carbon tax) decreases coal generation at an increasing rate. This marginal effect also becomes more negative because from 2008 to 2013, wind generation increased in all regions and all regions have a negative parameter on the interaction term $W * P^R$. A similar line of reasoning can be used to explain why the marginal effect of W on CF became more negative from 2008 to 2012.

Finally we also find, as shown in Table 4, that the "counterfactual" marginal effects in 2013 are generally of smaller magnitude than the 2013 "actual" marginal effects. Indeed, in some of these regions the disparity between the counterfactual and actual marginal effects is

[29] The standard errors (SEs) of the marginal effects are calculated based on treating the marginal effects as linear function of normally-distributed parameter estimates. Alternatively, one could bootstrap the SEs for the marginal effects. However, given the large sample sizes this was not feasible for all regions. We did calculate the bootstrapped SEs of the marginal effects for ERCOT and SPP. For these two regions, the bootstrapped SEs were smaller than those presented here.

quite large. For instance, in ERCOT, the marginal effect of wind generation W on capacity factor CF based on 2013 average values of W and P^R is approximately double what it would be in the counterfactual where natural gas prices remained high, such that P^R was its relatively low 2008-average level. Similarly, in SPP, the marginal effect of P^R on CF based on the 2013-average values of W and P^R is nearly three times larger than it would have been in the counterfactual where wind generation remained at its low 2008-average level.

The marginal effects at various price ratio and wind generation levels can be seen more completely in Figures 5 and 6. These figures give the marginal effect of P^R (Figure 5) and W (Figure 6) on CF over a range of P^R and W values in the form of a "heat map". In Figure 5, we show that for a given P^R value, the marginal effect of P^R increases in magnitude as the wind generation level increases for PJM, SPP, and to a lesser extent in ERCOT. The result is particularly stark in PJM, where we find that without some wind generation, we find little to no response of CF to P^R, but responses increase rather uniformly for any given P^R value as wind generation increase. On the other hand, results from MISO in Figure 5 show that while the marginal response of CF to P^R generally increases as P^R increases, these responses appear to remain constant as W increases.

In Figure 6, the results are more uniform across regions in that the marginal response of CF to W generally increases in magnitude as P^R increases. However, again for MISO, the range of marginal effects displayed is considerably narrower than what we see in other regions. The results shown in Figure 6 for ERCOT also largely confirm what has been found in Novan (2013), Cullen (2013) and Kaffine et al. (2013). These papers find little response of emissions to wind generation among coal plants in ERCOT using data from the mid-to-late-2000's. The P^R and W values in these years would correspond to the area in

the upper-left corner of the ERCOT plot in Figure 5, where we also find very little response of capacity factor, and therefore CO_2 emissions, to wind generation. However by 2013, P^R and W values are now in the lower-right portion of the ERCOT plot, where the response by coal generators is much larger in magnitude.

Turning to the marginal effects on emissions shown in Table 5, we find that the results follow the same basic patterns as those described above for CF. Again, largely significant marginal effects that become more negative from 2008 - 2013 and that have actual marginal effects that are more negative than the counterfactual effects. This is as expected given the correlation between capacity factors and CO_2 emissions per unit of capacity.[30]

The final aspect we consider among the quantile regression results is a comparison of the marginal effects across quantiles.[31] These comparisons are given in Table 6 for the CF specifications and in Table 7 for the E specifications. The tables present the marginal effects for each region based on using 2013-average values for P^R and W for quantile levels of $\tau = 0.25$, $\tau = 0.50$, and $\tau = 0.75$. Here we generally find that the marginal effects are declining in magnitude as the quantile increases.[32] This general pattern is in line with the expectations that the lower quantiles represent the less-efficient plants which typically run at lower capacity factors. These less-efficient plants will be more responsive to natural gas price declines and wind generation increases because they are more likely to be pushed off the margin. In ERCOT, the marginal effect of coal-to-natural gas price changes appears to

[30] Though not shown, the heat map displays of the marginal effects on CO_2 emissions also generally follow the same pattern as those shown in Figures 5 and 6.

[31] As illustrated in Section 2 and noted in Section 3.2, coal plants with varying marginal costs may be more or less responsive to changes in prices and wind generation.

[32] There are a few exceptions to this general finding, but in these instances the marginal effects across quantiles are not statistically different from one another. Note also that all marginal effects within an ISO region and across quantile levels are calculated using the same average values for P^R, and thus do not account for varying average input prices across quantiles.

be quite different across the lower and upper quantiles. This is expected given the relatively large proportion of natural gas-fired generation capacity in Texas, which provides for considerable reshuffling of the supply curve when relative fuel prices change. The other regions show considerably less variation in marginal effects across quantiles, suggesting relatively more homogeneous coal-fired units in these regions and/or less possibilities for considerable reshuffling of the supply curve.

4.2 Heckman 2-step Approach

Parameter estimates from the intensity equation given in (3) are given in Tables 8 and 9. For the specification with capacity factor as the dependent variable, we again find that all regions have a negative interaction effect between wind generation and the coal-to-natural gas price ratio, and are all statistically significant at at least the ten percent level. This again confirms the presence of a gas-wind interaction whereby higher wind generation levels will make coal-fired unit's net generation more responsive to P^R and vice-versa. For the specification with CO_2 emissions per unit of capacity, the parameter estimates again show an interaction effect that is negative across all regions, however the parameter is only statistically significant in PJM.

We again calculate the marginal effects, however, this calculation is slightly more complicated given that P^R and W appear in both the selection and intensity equations. The marginal effects are now:

$$\frac{\partial y_{it}}{\partial P_{it}^R} = \beta_1 + 2\beta_2 P_{it}^R + 3\beta_3 \left(P_{it}^R\right)^2 + \beta_7 W_t - \left(\gamma_1 + 2\gamma_2 P_{it}^R + 3\gamma_3 \left(P_{it}^R\right)^2 + \gamma_7 W_t\right) \beta_8 \delta_{it} \quad (6)$$

$$\frac{\partial y_{it}}{\partial W_t} = \beta 4_8 + 2\beta_5 W_t + 3\beta_6 W_t^2 + \beta_7 P_{it}^R - \left(\gamma_4 + 2\gamma_5 W_t + 3\gamma_6 W_t^2 + \gamma_7 P_{it}^R\right) \beta_8 \delta_{it} \quad (7)$$

where $\delta_{it} = \lambda_{it}^2 - \pi_{it}\lambda_{it}$ and π_{it} is again the propensity score associated with unit i running on day t. To calculate these marginal effects we use the estimated parameters along with estimated IMR ($\hat{\lambda}_{it}$) and propensity score ($\hat{\pi}_{it}$) values. Note also, because the marginal effects are a function of the estimated propensity scores and IMR's, one cannot readily form "counterfactual" marginal effects. We instead present 2008 and 2013 marginal effects for each region in Table 10. As with the marginal effects for the quantile estimation strategy, the "2008" effects are the marginal effects evaluated at the 2008 averages for all variables, including the IMR and propensity scores, in Equations (6) and (7). Likewise, the "2013" marginal effects are based on using the 2013 averages for all variables.

The upper half of Table 10 shows the marginal effects of CF with respect to P^R and W. These marginal effects generally follow the pattern of the median quantile regression estimates, with the magnitude of marginal effects increasing from 2008 to 2013. Furthermore, they are also quite similar in magnitude to the corresponding median quantile marginal effects.[33] The bottom half of Table 10 reports the marginal effects for CO_2 emissions per unit of capacity. Again, these results generally follow the pattern of their counterparts in the median quantile marginal effects, though the differences between the 2008 to 2013 effects are slightly narrower under the two-step approach.

Overall, the results from the Heckman two-step method provide further evidence of the robustness of our general finding of a significant interaction effect, as well as to the approximate size of this effect. Beyond this robustness check, we also considered several other specifications. Of note, we ran estimations where instead of using $Load_{it}$ as an independent

[33] The only somewhat notable discrepancy is for MISO results, where the estimate for the marginal effect with respect to W decreases in magnitude from 2008 to 2013. However, the point estimates for the two years are within two standard deviations of each other.

variable, we instead included transmission zone electricity prices, $pricemwh_{it}$. The variable $pricemwh_{it}$ is likely to be endogenous due to a simultaneity bias, and thus we instrumented for $pricemwh_{it}$ with $Load_{it}$ and $Load_{it}^2$. The results of the parameter estimates and marginal effects were not materially different for either estimation procedure than what is shown here. Because we are using data at the generating unit level, we also considered specifications that allowed coal-fired units in plants that also had natural gas-fired units to have a different response from those units in plants with only coal-fired units. Results from this specification did show that units in plants that also have natural gas-fired units are somewhat more responsive to P^R and W. However, the differences between the responses of these two groups (those in plants with only coal-fired units and those in plants with coal- and natural gas-fired units) were not significantly different from one another and, again, the results of the marginal effects were not materially different than what is shown here.

5 Policy Simulation

With the recent proposal of the EPA's Clean Power Plan (CPP), some form of carbon pricing appears more likely for the power generation sector. At the same time, the phasing out of the federal production tax credit for wind generation and calls at the state-level for repeals of existing renewable portfolio standards stand as limiting factors for the growth of wind generation in the U.S. Given the variation in coal-to-natural gas price ratios and wind generation levels, the analysis presented above is well suited to see how variation in future carbon pricing systems, which effectively alter the fuel-price ratio, and wind generation levels will affect coal-fired units. In particular, we are interested in whether or not overlapping

policies such as carbon pricing and policies that increase wind capacity are complements or substitutes in terms of their impact on coal-fired generation. Therefore, in this section, we use the estimated parameters from above to conduct a simple "back of the envelope" policy analysis in an effort to show the effect of carbon pricing under various wind generation growth assumptions for the four regions examined.

5.1 Simulation assumptions

To start, we obtain projections of natural gas and coal prices in 2020, the year the CPP is scheduled to begin, from the Energy Information Administration's 2014 Annual Energy Outlook (2014AEO) reference case scenario. The projected prices are \$5.07/MMBtu and \$2.61/MMBtu for natural gas and coal, respectively, for a coal-to-natural gas price ratio of about 0.5, well within our observed range.[34] Based on these prices, average daily wind generation levels from 2013 for each ISO, and our parameter estimates from the median quantile regression results, we predict capacity factor and CO_2 emissions per unit capacity levels. Next, we assume various levels of a tax on CO_2 emissions, and based on each regions average emission rates (tons CO_2 emissions per MWh of generation) and heat rates (MMBtu of fuel burned per MWh of generation) for natural gas- and coal-fired units, form an updated coal-to-natural gas price ratio. We also generate new daily average wind generation levels for each region by assuming wind generation growths of 30%, 50%, and 100%, with 30% reflecting the 2014AEO's nation-wide predicted growth in wind generation for 2020.[35]

[34] Note that the 2014AEO's reference case scenario does not include provisions of the CPP.

[35] Note that we have a high degree of variance in our daily wind generation for each region. Thus, while 100% wind growth from 2013 averages are quite large and may raise concerns about predicting out of sample, we do observe days in our sample that meet this level. Furthermore, while assuming 100% wind generation growth by 2020 may seem aggressive, it is worth noting that this growth rate is slower than the observed growth rates over the last five years in these regions.

Given these updated fuel price ratios and scale of assumed wind generation growth levels, we again predict a set of capacity factors and CO_2 emissions levels. To obtain a sense of the changes in coal-fired unit operations relative to a "no carbon pricing - no wind growth" scenario, we then calculate the difference between predicted capacity factor and emissions levels and their counterparts under the assumption of no carbon pricing and 2013 average wind generation levels. The results of this policy analysis are plotted in Figures 7 and 8. More formally, defining $CF(P_x^{CO2}, W_y)$ as the predicted capacity factor for a given region under a carbon price of x and assuming wind generation is y% bigger than the 2013 daily average, Figure 7 plots $CF(P_x^{CO2}, W_y) - CF(P_0^{CO2}, W_0)$ for values of x from \$0/tCO_2 to \$50/tCO_2 and y at 0%, 30%, 50%, and 100%. Figure 8 is formed analogously.

5.2 Simulation results

In Figure 7, we see that the various wind growth curves have different intercepts at the zero-carbon price point. These intercepts pick up the capacity factor reductions, relative to the no carbon pricing - no wind growth baseline, that are due strictly to differences in assumed wind generation growth. All wind growth scenarios show declining relative capacity factors as the carbon tax increases, which is expected as increasing carbon taxes increase P^R. These declines in capacity factor are quite large in some regions. For example, in ERCOT and MISO at a carbon tax of \$30/tCO_2, we find capacity factors drop in the range of 8 to 15 percentage points depending upon the wind generation growth assumptions. One can also see that the higher the assumed wind generation growth, the greater the reduction in capacity factor predicted for a given carbon tax level. The scenarios that assume a higher

wind generation level start at a lower relative capacity factor when carbon taxes are zero, so we would expect that we would have more capacity factor reductions at higher wind growth assumptions for a given tax. However, the figure also shows that the plotted curves in SPP and PJM, and to a lesser extent in ERCOT, "fan-out" as the carbon tax increases. The increasing spread across the curves as the carbon tax increases is due to the interaction effect, and this effect is quite large in percentage terms in some regions. For example, in SPP, a 100% wind growth assumption drops capacity factor by about 6 percentage points with no carbon pricing. At a carbon tax of \$30/tCO_2, the gap between the "Wind Growth = 0%" and "Wind Growth = 100%" curves is about 10 percentage points. This means that the interaction effect at that carbon tax level and that assumed wind growth leads to an additional 4 percentage points reduction in capacity factors, or 40% of the total observed additional reductions in capacity factors.[36] On the other end of the spectrum, the gap between the "Wind Growth = 0%" curve and other curves for the MISO panel remains relatively constant as the carbon tax increases. This is as expected since we found little evidence of a significant interaction effect in MISO.

For the CO_2 emission reduction plots shown in Figure 8, we converted the predicted CO_2 emissions per unit capacity prediction values to simply CO_2 emissions (in tCO_2) by multiplying the predicted values by the given region's average coal-fired unit capacity. The general patterns of the plots in Figure 8 follow that of Figure 7. It should also be noted that while the reductions in CO_2 emissions might seem somewhat small, for example in ERCOT we predict a relative drop in emissions under a \$30/tCO_2 tax in the range of about 1300 to

[36] Even at the modest 30% wind growth level, the interaction effect makes up a large share of the additional capacity factor reduction we see from having wind growth and a carbon tax. For example, in SPP at a \$30/tCO_2, the interaction effect accounts for about 33% of the observed difference between the zero-wind growth and 30%-wind growth plots.

2000tCO_2/day, it is important to remember these are per-unit, daily average reductions.[37] The role of the interaction effect is also quite apparent, particularly in the fanning-out of the plots seen for PJM. For instance, at a tax of \$30/tCO2, the gap between the 0% and 100% wind growth curves is about 220tCO_2/day for PJM. Given the initial gap between these curves in PJM, the interaction effect is accounting for, on average, about an extra 130tCO_2/day per unit. Using the EPAs 2020 social cost of carbon of \$46/tCO_2, the annual value of the interaction effect at a \$30/tCO2 tax and a 100% wind growth assumption is about \$490 million.[38] In ERCOT and SPP the size of the interaction effect at a tax of \$30/tCO2 and when comparing the 100% wind growth to the 0% growth case is similar to PJM, about 200tCO_2/day per unit. Again, this suggests the potential for an economically significant value of the interaction.

5.3 Further discussion

As we note above, some plants may not report direct measurement of CO_2 emissions to CEMS, but rather have their emissions imputed based on their fuel use. As an alternative approach to calculating CO_2 reductions, we also calculate implied emissions reductions for the policy scenarios above based on the capacity factor reductions. More specifically, we take the calculated relative CF reductions shown in Figure 7, and multiply these values by the given region's average unit capacity to produce an average net generation reduction value. We then multiply this net generation reduction value by the region's average CO_2 emissions

[37] It is also worth noting that the magnitude of the relative emissions reductions in ERCOT are considerably larger than in other regions. This is due mainly to the fact that the average coal-fired unit capacity in ERCOT is considerably larger than in other regions.

[38] The \$46/tCO_2 is a 2011-dollars value based on the EPAs 3% discounting rate scenario. Details can be found at http://www.epa.gov/climatechange/EPAactivities/economics/scc.html.

rate (tCO_2/MWh). Results from this method are shown in Figure 9. Relative emission reductions presented in Figure 9 are noticeably larger than those presented in Figure 8 and generally imply stronger interaction effects. The differences between the figures could arise for several reasons. For instance, emissions reporting errors may obscure our results using the emission values directly from CEMS.[39] However, the magnitude of the discrepancies between the figures for each region would imply a rather implausibly large reporting error if that is the source of the difference. Alternatively, using the CF results to impute emission reduction may overstate emission reductions because as units operate at lower capacity factors, their decreasing thermal efficiency can also lead to higher emission rates. There are also more shutdowns and re-starts of the coal-fired units under higher P^R and W values, which will also lead to higher observed average emission rates relative to the imputed levels. Taken together, this suggests that while we show carbon taxes combined with relatively large wind generation levels can significantly reduce capacity factors of coal-fired units, the resulting emission reductions may not be as large as these CF reductions would imply due to higher emission rates associated with lower capacity factors.

Finally, the policy analysis above is quite simple and a few caveats of this analysis are worth mentioning. First we do not assume any general equilibrium effects, so, for example, reductions in coal-fired units capacity factors does not affect coal or natural gas prices. Such fuel price general equilibrium effects are likely not a major issue here as coal can be sold on global markets and large gas reserves are available to increase supply should generation mixes shift heavily to natural gas fired plants. A more limiting restriction is that we do

[39] Reporting errors in net generation, and therefore capacity factor, are much less likely given that ISO's must directly monitor generation at all points in time to maintain a constant supply and demand balance.

not assume any plant retirements. Given our predicted reduction in capacity factors under higher carbon taxes, it is likely that many coal plants would be forced to shut down. A change in the generation capacity would likely lead to different marginal responses to fuel price and wind generation changes and thus alter our predictions. However, we can use pre-existing differences in generation capacities across ISOs to perhaps shed some light on what a region's response may look like if its capacity mix changes. For example, MISO is quite coal dominated, but if it has many closures in coal plants, it will start to resemble SPP or ERCOT in terms of capacity mix. Therefore, the estimates in these regions may serve as a basis for predicted responses in MISO in a more dynamic model that allows closures.

6 Conclusion

In this preceding sections, we examine the joint impact of the dramatic fall in natural gas prices and the substantial increase in wind generation on coal-fired generation and CO_2 emissions. Consistent with prior research, we find that lower natural gas prices have decreased coal-fired generation and emissions (Cullen and Mansur 2013; Linn et al. 2014; Holladay and LaRiviere 2014; Linn et al. 2014). Similarly, increased wind generation has also decreased coal-fired generation and emissions (Novan 2013; Cullen 2013; Kaffine et al. 2013). Importantly though, we also find an effect not considered in these related papers, specifically a statistically and economically significant interaction effect between fuel prices and wind generation in most regions. The interaction effect shows that cheaper natural gas and greater wind generation levels together lead to a greater reduction in coal-fired generation and emissions than either factor in isolation. The magnitude of this interaction effect is

substantial, and in some regions, marginal responses of coal-fired generation to natural gas prices in 2013 were several times what they would have been had wind generation remained at 2008 levels. Similar sensitivities were found for responses to wind generation had natural gas prices remained at 2008 levels.

Our exploration of the effects of carbon pricing coupled with policies to promote wind growth find that such policies would be complementary due to the presence of the interaction effect. While previous literature on overlapping policies has emphasized the potential for reduced policy effectiveness due to "leakage," our findings highlight the importance of considering production-side complementarities. Analysis that failed to account for interactions between natural gas and wind may understate the potential benefits of carbon pricing.

While our analysis provides insight into the evolution of the electricity sector over the last few years as well as potential impacts of future policies, a few caveats are in order. First, data limitations restricted the scope of our analysis to only a subset of the United States. And while the regions considered represent a considerable fraction of US population and wind generation, further research incorporating other areas of the US may be beneficial. Second, while we focus on coal-fired generation, additional research examining the complementary relationship between wind and gas may provide further insight into how various policies under consideration will impact the electricity sector. Finally, while we focus on the short-run operating margin, there may be important effects of natural gas prices and wind generation growth on longer-run build decisions that warrant further inquiry.

References

Amor, M. B., E. Billette de Villemeur, M. Pellat, and P.-O. Pineau (2014). Influence of wind power on hourly electricity prices and GHG emissions: Evidence that congestion

matters from Ontario zonal data. *Working Paper*.

Atkinson, S. E. and R. Halvorsen (1976). Interfuel substitution in steam electric power generation. *Journal of Political Economy 84*(5), 959–78.

Böhringer, C., H. Koschel, and U. Moslener (2008). Efficiency losses from overlapping regulation of EU carbon emissions. *Journal of Regulatory Economics 33*(3), 299–317.

Böhringer, C. and K. E. Rosendahl (2010). Green promotes the dirtiest: On the interaction between black and green quotas in energy markets. *Journal of Regulatory Economics 37*(3), 316–325.

Bopp, A. E. and D. Costello (1990). The economics of fuel choice at US electric utilities. *Energy Economics 12*(2), 82–88.

Bushnell, J., Y. Chen, and M. Zaragoza-Watkins (2014). Downstream regulation of CO2 emissions in California's electricity sector. *Energy Policy 64*, 313–323.

Callaway, D. and M. Fowlie (2009). Greenhouse gas emissions reductions from wind energy: Location, location, location? *Working paper*.

Cullen, J. (2013). Measuring the environmental benefits of wind-generated electricity. *American Economic Journal: Economic Policy 5*(4), 107–133.

Cullen, J. A. and E. T. Mansur (2013). Will carbon prices reduce emissions in the US electricity industry? Evidence from the shale gas experience. *Working Paper*.

Denholm, P., G. L. Kulcinski, and T. Holloway (2005). Emissions and energy efficiency assessment of baseload wind energy systems. *Environmental Science and Technology 39*, 1903–1911.

Fell, H. and J. Linn (2013). Renewable electricity policies, heterogeneity, and cost effectiveness. *Journal of Environmental Economics and Management 66*(3), 688–707.

Fernández-Val, I. (2009). Fixed effects estimation of structural parameters and marginal effects in panel probit models. *Journal of Econometrics 150*(1), 71–85.

Fernández-Val, I. and F. Vella (2011). Bias corrections for two-step fixed effects panel data estimators. *Journal of Econometrics 163*(2), 144–162.

Fischer, C. and R. G. Newell (2008). Environmental and technology policies for climate mitigation. *Journal of Environmental Economics and Management 55*(2), 142–162.

Fischer, C. and L. Preonas (2010). Combining policies for renewable energy: Is the whole less than the sum of its parts. *International Review of Environmental and Resource Economics 4*(1), 51–92.

Galvao, A. F., C. Lamarche, and L. Lima (2013). Estimation of censored quantile regression for panel data with fixed effects. *Journal of the American Statistical Association 108*, 1075–1089.

Godby, R., G. L. Torell, and R. Coupal (2013). Estimating the value of additional wind and transmission capacity in the Rocky Mountain West. *Resource and Energy Economics 36*(1), 22–48.

Goulder, L. H., M. R. Jacobsen, and A. A. Van Benthem (2012). Unintended consequences from nested state and federal regulations: The case of the Pavley greenhouse-gas-per-mile limits. *Journal of Environmental Economics and Management 63*(2), 187–207.

Goulder, L. H. and R. N. Stavins (2011). Challenges from state-federal interactions in US climate change policy. *American Economic Review 101*(3), 253–257.

Griffin, J. M. (1977). Inter-fuel substitution possibilities: A translog application to inter-country data. *International Economic Review 18*(3), 755–70.

Heckman, J. J. (1979). Sample selection bias as a specification error. *Econometrica 47*, 153–161.

Holladay, J. S. and J. LaRiviere (2014). The effect of abundant natural gas on air pollution from electricity production. *Working Paper*.

Holttinen, H. and S. Tuhkanen (2004). The effect of wind power on CO2 abatement in the Nordic countries. *Energy Policy 32*(14), 1639–1652.

Joskow, P. L. (2011). Comparing the costs of intermittent and dispatchable electricity generating technologies. *American Economic Review 101*(3), 238–241.

Joskow, P. L. (2013). Natural gas: From shortages to abundance in the United States. *American Economic Review 103*(3), 338–343.

Joskow, P. L. and F. S. Mishkin (1977). Electric utility fuel choice behavior in the United States. *International Economic Review 18*(3), 719–736.

Kaffine, D. T., B. J. McBee, and J. Lieskovsky (2013). Emissions savings from wind power generation in Texas. *Energy Journal 34*(1), 155–175.

Katzenstein, W. and J. Apt (2009). Air emissions due to wind and solar power. *Environmental Science and Technology 43*(2), 253–258.

Kubik, M., P. Coker, and C. Hunt (2012). The role of conventional generation in managing variability. *Energy Policy 50*, 253–261.

Lafrancois, B. A. (2012). A lot left over: Reducing CO2 emissions in the United States' electric power sector through the use of natural gas. *Energy Policy 50*, 428–435.

Levinson, A. (2010). Belts and suspenders: Interactions among climate policy regulations. Technical report, National Bureau of Economic Research.

Linn, J., E. Mastrangelo, and D. Burtraw (2014). Regulating greenhouse gases from coal power plants under the Clean Air Act. *Journal of the American Environmental and Resource Association*, Forthcoming.

Linn, J., L. Muehlenbachs, and Y. Wang (2014). How do natural gas prices affect electricity consumers and the environment? *RFF Working Paper DP 14-19*.

Lu, X., J. Salovaara, and M. B. McElroy (2012). Implications of the recent reductions in natural gas prices for emissions of CO2 from the US power sector. *Environmental Science & Technology 46*(5), 3014–3021.

Newcomer, A., S. A. Blumsack, J. Apt, L. B. Lave, and M. G. Morgan (2008). Short run effects of a price on carbon dioxide emissions from US electric generators. *Environmental Science & Technology 42*(9), 3139–3144.

Novan, K. M. (2013). Valuing the wind: Renewable energy policies and air pollution avoided. *UC Center for Energy and Environmental Economics Working Paper Series E^3 WP-027*.

Pettersson, F., P. Söderholm, and R. Lundmark (2012). Fuel switching and climate and energy policies in the european power generation sector: A generalized leontief model. *Energy Economics 34*(4), 1064–1073.

Roth, K. (2014). The unintended consequences of uncoordinated regulation: Evidence from the transportation sector. *Working paper*.

Schmalensee, R. (2012). Evaluating policies to increase electricity generation from renewable energy. *Review of Environmental Economics and Policy 6*(1), 45–64.

Soloway, S. (2013). Fuel switching and human health: Moving from oil to natural gas at New York City electricity generating facilities. *Working Paper*.

Traber, T. and C. Kemfert (2011). Gone with the wind? Electricity market prices and incentives to invest in thermal power plants under increasing wind energy supply. *Energy Economics 33*(2), 249–256.

Wooldridge, J. M. (2002). *Econometric Analysis of Cross Section and Panel Data*. Cambridge, MA: The MIT Press. chapter 16.

Table 1: Data Summary

	ERCOT				MISO			
	Mean	SD	Mean-2008	Mean-2013	Mean	SD	Mean-2008	Mean-2013
CF	0.730	0.301	0.788	0.706	0.542	0.343	0.620	0.495
E	0.818	0.339	0.902	0.791	0.655	0.385	0.762	0.587
P^R	0.496	0.198	0.222	0.553	0.519	0.228	0.306	0.579
W	0.694	0.384	0.416	0.896	0.625	0.432	0.232	0.969
$Load$	278198	85918	268226	286543	84123	57336	84944	85614

	PJM				SPP			
	Mean	SD	Mean-2008	Mean-2013	Mean	SD	Mean-2008	Mean-2013
CF	0.486	0.365	0.597	0.435	0.643	0.302	0.707	0.614
E	0.512	0.384	0.618	0.466	0.737	0.346	0.826	0.698
P^R	0.662	0.291	0.381	0.716	0.429	0.169	0.287	0.465
W	0.261	0.196	0.094	0.403	0.374	0.259	0.162	0.697
$Load$	216029	136405	247614	215562	54246	39564	53026	56441

Notes: Columns "Mean" and "SD" give the regional mean and standard deviation, respectively, of the variables over the entire sample. "Mean-2008" and "Mean-2013" give the regional mean of the variables for years 2008 and 2013, respectively

Table 2: Capacity Factor Results - Median Quantile

	ERCOT	MISO	PJM	SPP
P^R	0.235	0.209**	-0.0543**	0.0490
	(0.228)	(0.0970)	(0.026)	(0.0776)
$\left(P^R\right)^2$	-0.594*	-0.581***	-0.007	-0.0751
	(0.308)	(0.164)	(0.012)	(0.0784)
$\left(P^R\right)^3$	0.253**	0.264***	0.001	0.00832
	(0.108)	(0.0794)	(0.001)	(0.00782)
W	0.007	-0.0278***	0.070***	0.034*
	(0.012)	(0.00642)	(0.023)	(0.020)
W^2	-0.023	0.00850	-0.0001	-0.034
	(0.016)	(0.00787)	(0.037)	(0.032)
W^3	0.011**	-0.00507**	-0.021	0.014
	(0.005)	(0.00249)	(0.031)	(0.016)
$P^R * W$	-0.080**	-0.0166	-0.120***	-0.189***
	(0.032)	(0.0158)	(0.0306)	(0.066)
Age	0.0010	-0.00105	-0.001	0.0002
	(0.0017)	(0.000686)	(0.001)	(0.0004)
Load	1.21e-06***	2.44e-06***	2.87e-06***	4.03e-06***
	(2.45e-07)	(7.60e-07)	(2.50e-07)	(4.37e-07)
$Load^2$	-0***	-0	-0***	-0***
	(0)	(0)	(0)	(0)
Obs	55,014	349,316	254,332	125,430
N	30	204	162	68

*Notes: "Obs" gives total number of observations and "N" denotes number of cross-sectional units included in the quantile regression for year 2013. Standard errors (SEs) are given in brackets. SEs are clustered at the unit level for all ISO's except NYISO due to its small N. * indicates 10 percent significance.** indicates 5 percent significance. *** indicates 1 percent significance.*

Table 3: CO_2 Emission Results - Median Quantile

	ERCOT	MISO	PJM	SPP
P^R	-0.147	0.107	-0.0576**	0.122
	(0.253)	(0.139)	(0.0275)	(0.109)
$\left(P^R\right)^2$	-0.192	-0.382	-0.0006	-0.152
	(0.307)	(0.248)	(0.0153)	(0.105)
$\left(P^R\right)^3$	0.129	0.163	0.0009	0.0156
	(0.0996)	(0.120)	(0.0015)	(0.0104)
W	-0.0220*	-0.0401***	0.0659***	-0.0025
	(0.0133)	(0.00841)	(0.0195)	(0.0263)
W^2	-0.0112	0.0160*	0.0019	-0.0316
	(0.0180)	(0.00911)	(0.0309)	(0.0297)
W^3	0.0074	-0.00748***	-0.0275	0.0127
	(0.0060)	(0.00278)	(0.0216)	(0.0141)
$P^R * W$	-0.0479*	-0.0150	-0.112***	-0.124*
	(0.0245)	(0.0203)	(0.0301)	(0.0731)
Age	-0.0052	-0.000141	-0.0030***	0.0049***
	(0.0040)	(0.000209)	(0.0003)	(0.0005)
Load	1.50e-06***	2.71e-06**	3.80e-05***	4.14e-06***
	(2.47e-07)	(1.06e-06)	(5.75e-06)	(5.20e-07)
$Load^2$	-0***	-0	-2.66e-10***	-0***
	(0)	(0)	(6.40e-11)	(0)
Obs	55,014	364,327	259,743	125,430
N	30	206	164	68

*Notes: *, **, *** denote statistical significance at at least the 10, 5, and 1 percent levels, respectively. Standard errors are given in parentheses below the parameter estimates. "Obs" given total number of observations. "N" denotes the number of cross-sectional units used in the quantile regression in 2013.*

Table 4: Quantile Median Marginal Effects for Capacity Factor

$\frac{\partial CF}{\partial P^R}$ Results								
	ERCOT		MISO		PJM		SPP	
	Actual	W2008	Actual	W2008	Actual	W2008	Actual	W2008
2008	-0.018	-0.018	-0.064	-0.064	-0.070	-0.070	-0.022	-0.022
	(0.110)	(0.110)	(0.031)	(0.031)	(0.019)	(0.019)	(0.036)	(0.036)
2013	-0.254	-0.216	-0.201	-0.189	-0.110	-0.073	-0.147	-0.046
	(0.065)	(0.057)	(0.019)	(0.022)	(0.016)	(0.015)	(0.045)	(0.023)

$\frac{\partial CF}{\partial W}$ Results								
	ERCOT		MISO		PJM		SPP	
	Actual	P2008	Actual	P2008	Actual	P2008	Actual	P2008
2008	-0.023	-0.023	-0.030	-0.030	0.023	0.023	-0.030	-0.030
	(0.007)	(0.007)	(0.003)	(0.003)	(0.011)	(0.011)	(0.009)	(0.009)
2013	-0.045	-0.019	-0.039	-0.034	-0.027	0.014	-0.077	-0.043
	(0.006)	(0.010)	(0.003)	(0.006)	(0.005)	(0.012)	(0.007)	(0.012)

Notes: "2008" rows refer to marginal effects calculated using 2008 variable averages. "2013" rows refer to marginal effects calculated using 2013 variable averages. "Actual" columns refer to marginal effects calculated using the variable averages from the year stated in the first column. "W2008" columns holds W at 2008 averages in the calculation of the marginal effect. Standard errors are given in parentheses below the calculated marginal effects. "P2008" columns holds P^R at 2008 averages in the calculation of the marginal effect. Standard errors are given in parentheses below the calculated marginal effects.

Table 5: Quantile Median Marginal Effects for CO_2 Emissions

$\frac{\partial E}{\partial P^R}$ Results

	ERCOT		MISO		PJM		SPP	
	Actual	W2008	Actual	W2008	Actual	W2008	Actual	W2008
2008	-0.342	-0.342	-0.089	-0.089	-0.080	-0.080	0.058	0.058
	(0.142)	(0.142)	(0.036)	(0.036)	(0.027)	(0.027)	(0.049)	(0.049)
2013	-0.403	-0.374	-0.186	-0.172	-0.098	-0.076	-0.074	-0.013
	(0.050)	(0.045)	(0.023)	(0.029)	(0.018)	(0.015)	(0.057)	(0.031)

$\frac{\partial E}{\partial W}$ Results

	ERCOT		MISO		PJM		SPP	
	Actual	P2008	Actual	P2008	Actual	P2008	Actual	P2008
2008	-0.037	-0.037	-0.038	-0.038	0.023	0.023	-0.047	-0.047
	(0.008)	(0.008)	(0.004)	(0.004)	(0.010)	(0.010)	(0.012)	(0.012)
2013	-0.046	-0.030	-0.043	-0.038	-0.027	0.011	-0.082	-0.060
	(0.007)	(0.010)	(0.003)	(0.007)	(0.005)	(0.013)	(0.008)	(0.015)

Notes: "2008" rows refer to marginal effects calculated using 2008 variable averages. "2013" rows refer to marginal effects calculated using 2013 variable averages. "Actual" columns refer to marginal effects calculated using the variable averages from the year stated in the first column. "W2008" columns holds W at 2008 averages in the calculation of the marginal effect. Standard errors are given in parentheses below the calculated marginal effects. "P2008" columns holds P^R at 2008 averages in the calculation of the marginal effect. Standard errors are given in parentheses below the calculated marginal effects.

Table 6: Quantile Comparison for Capacity Factors

	$\frac{\partial CF}{\partial P^R}$ Comparison				$\frac{\partial CF}{\partial W}$ Comparison			
	ERCOT	MISO	PJM	SPP	ERCOT	MISO	PJM	SPP
$\tau = 0.25$	-0.388	-0.204	-0.113	-0.107	-0.061	-0.053	-0.033	-0.105
	(0.072)	(0.023)	(0.017)	(0.056)	(0.010)	(0.005)	(0.006)	(0.016)
$\tau = 0.50$	-0.254	-0.201	-0.110	-0.147	-0.045	-0.039	-0.027	-0.077
	(0.065)	(0.019)	(0.016)	(0.045)	(0.006)	(0.003)	(0.005)	(0.007)
$\tau = 0.75$	-0.161	-0.174	-0.098	-0.125	-0.029	-0.031	-0.023	-0.053
	(0.070)	(0.019)	(0.013)	(0.046)	(0.005)	(0.002)	(0.004)	(0.009)

Table 7: Quantile Comparison for CO_2 Emissions

	$\frac{\partial E}{\partial P^R}$ Comparison				$\frac{\partial E}{\partial W}$ Comparison			
	ERCOT	MISO	PJM	SPP	ERCOT	MISO	PJM	SPP
$\tau = 0.25$	-0.403	-0.204	-0.098	-0.074	-0.065	-0.061	-0.031	-0.109
	(0.050)	(0.023)	(0.018)	(0.057)	(0.009)	(0.006)	(0.006)	(0.013)
$\tau = 0.50$	-0.280	-0.201	-0.102	-0.095	-0.046	-0.043	-0.027	-0.082
	(0.044)	(0.019)	(0.015)	(0.051)	(0.007)	(0.003)	(0.005)	(0.008)
$\tau = 0.75$	-0.228	-0.174	-0.092	-0.082	-0.039	-0.034	-0.025	-0.065
	(0.041)	(0.019)	(0.014)	(0.049)	(0.008)	(0.002)	(0.004)	(0.008)

Table 8: Capacity Factor Results - two-step Method

	ERCOT	MISO	PJM	SPP
P^R	0.192	-0.0789	-0.114***	0.0343
	(0.262)	(0.0799)	(0.0232)	(0.0944)
$\left(P^R\right)^2$	-0.596*	-0.123	0.0277**	-0.160
	(0.340)	(0.124)	(0.0110)	(0.119)
$\left(P^R\right)^3$	0.261**	0.0666	-0.00146	0.0598
	(0.120)	(0.0592)	(0.000944)	(0.0399)
W	-0.00714	-0.0370***	0.0734***	-0.0451*
	(0.0133)	(0.00688)	(0.0211)	(0.0266)
W^2	-0.0351	0.0223**	-0.0654	0.0302
	(0.0225)	(0.00948)	(0.0433)	(0.0383)
W^3	0.0151*	-0.00755**	0.0281	-0.0165
	(0.00815)	(0.00301)	(0.0313)	(0.0176)
$P^R * W$	-0.0463*	-0.0254*	-0.0960***	-0.122*
	(0.0250)	(0.0135)	(0.0232)	(0.0682)
Age	0.00334	1.49e-05	0.000724	-
	(0.00216)	(0.000688)	(0.00130)	-
$Load$	1.57e-06***	2.24e-06***	2.68e-06***	4.00e-06***
	(2.18e-07)	(4.62e-07)	(1.93e-07)	(5.11e-07)
$Load^2$	-0***	-0*	-0***	-0***
	(0)	(0)	(0)	(0)
Obs	57,725	359,139	280,937	106,710
N	32	226	228	68

*Notes: "Obs" gives total number of observations and "N" denotes number of cross-sectional units included in the quantile regression for year 2013. Standard errors (SEs) are given in brackets. SEs are clustered at the unit level for all ISO's. The variable "Age" was dropped for SPP due to collinearity. * indicates 10 percent significance.** indicates 5 percent significance. *** indicates 1 percent significance.*

Table 9: CO_2 Emission Results - two-step Method

	ERCOT	MISO	PJM	SPP
P^R	-0.147	-0.107	-0.057**	0.209
	(0.244)	(0.093)	(0.029)	(0.148)
$\left(P^R\right)^2$	-0.245	-0.118	0.006	-0.282
	(0.310)	(0.143)	(0.014)	(0.176)
$\left(P^R\right)^3$	0.158	0.064	0.0002	0.063
	(0.107)	(0.069)	(0.0012)	(0.065)
W	-0.025	-0.054***	0.037	-0.055*
	(0.018)	(0.009)	(0.023)	(0.028)
W^2	-0.034	0.023**	-0.048	0.004
	(0.029)	(0.011)	(0.044)	(0.037)
W^3	0.015	-0.008**	0.013	-0.005
	(0.011)	(0.004)	(0.032)	(0.017)
$P^R * W$	-0.024	-0.010	-0.059**	-0.080
	(0.024)	(0.016)	(0.025)	(0.070)
Age	-0.003	-0.001	-0.0001	
	(0.005)	(0.001)	(0.002)	
$Load$	1.82e-06***	2.80e-06***	3.13e-06***	4.96e-06***
	(2.65e-07)	(5.37e-07)	(2.03e-07)	(5.11e-07)
$Load^2$	-0***	-0*	-0***	-0***
	(0)	(0)	(0)	(0)
Obs	57,752	359,124	289,336	125,375
N	32	226	226	69

*Notes: "Obs" gives total number of observations and "N" denotes number of cross-sectional units included in the quantile regression for year 2013. Standard errors (SEs) are given in brackets. SEs are clustered at the unit level for all ISO's. The variable "Age" was dropped for SPP due to collinearity. * indicates 10 percent significance.** indicates 5 percent significance. *** indicates 1 percent significance.*

Table 10: Two-step Method Marginal Effects

	ERCOT		MISO		PJM		SPP	
	$\partial CF/\partial P^R$	$\partial CF/\partial W$	$\partial CF/\partial P^R$	$\partial CF/\partial W$	$\partial CF/\partial P^R$	$\partial CF/\partial W$	$\partial CF/\partial P^R$	$\partial CF/\partial W$
2008	-0.035	-0.039	-0.140	-0.034	-0.099	0.020	0.003	-0.067
	(0.163)	(0.009)	(0.033)	(0.004)	(0.017)	(0.011)	(0.040)	(0.012)
2013	-0.264	-0.061	-0.174	-0.027	-0.111	-0.032	-0.121	-0.079
	(0.080)	(0.008)	(0.022)	(0.004)	(0.013)	(0.005)	(0.041)	(0.009)

	ERCOT		MISO		PJM		SPP	
	$\partial E/\partial P^R$	$\partial E/\partial W$	$\partial E/\partial P^R$	$\partial E/\partial W$	$\partial E/\partial P^R$	$\partial E/\partial W$	$\partial E/\partial P^R$	$\partial E/\partial W$
2008	-0.236	-0.051	-0.167	-0.047	-0.047	0.005	0.049	-0.081
	(0.153)	(0.009)	(0.037)	(0.005)	(0.021)	(0.013)	(0.072)	(0.014)
2013	-0.290	-0.064	-0.189	-0.036	-0.062	-0.037	-0.066	-0.094
	(0.067)	(0.010)	(0.025)	(0.004)	(0.015)	(0.007)	(0.054)	(0.011)

Notes:Marginal effects are inclusive of the effect of variables on the inverse Mills ratio. "2008" rows refer to marginal effects calculated using 2008 variable averages. "2013" rows refer to marginal effects calculated using 2013 variable averages. Bootstrapped standard errors are given in parentheses below the marginal effect estimates.

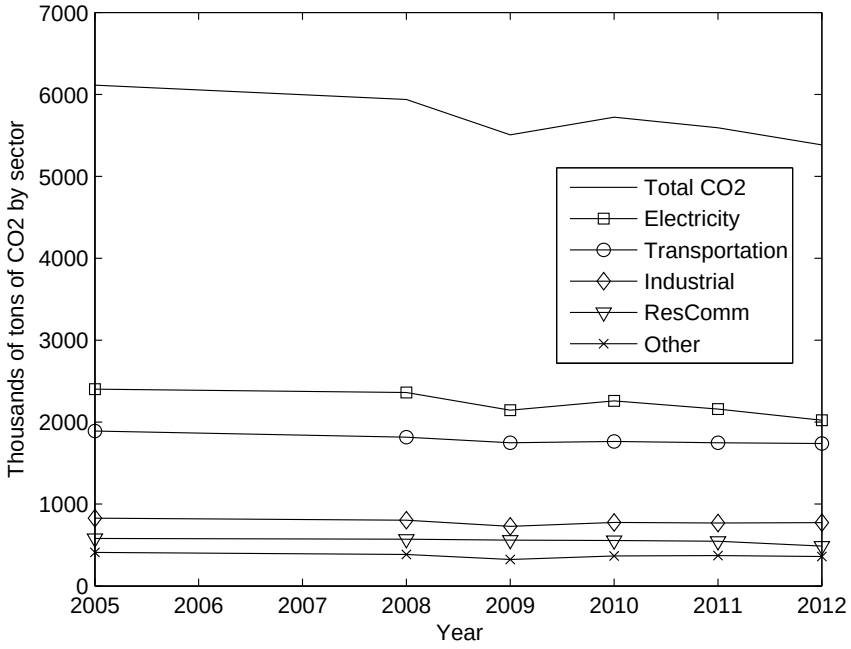

Figure 1: CO2 emissions by sector. Source: EPA

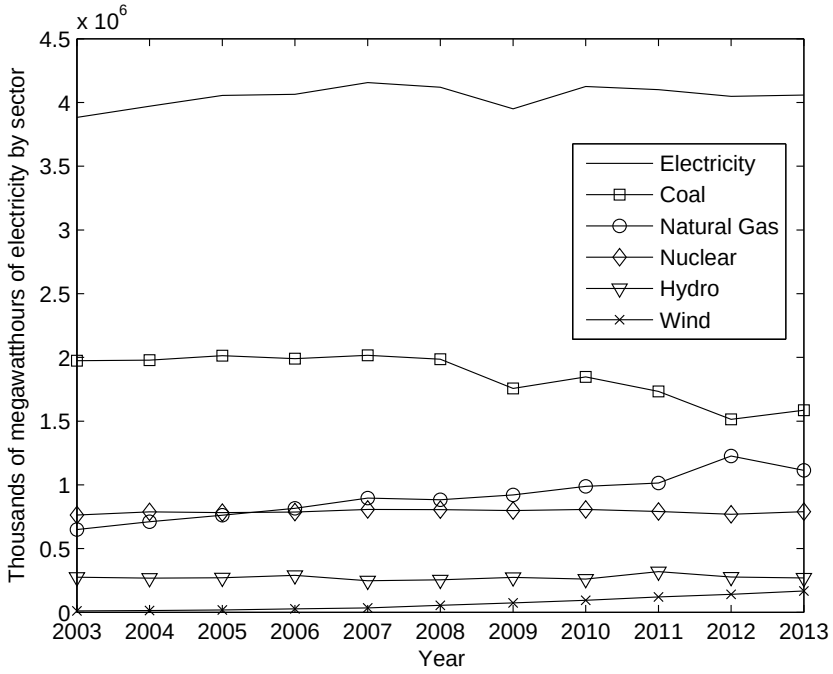

Figure 2: Electricity Generation by sector. Source: EIA

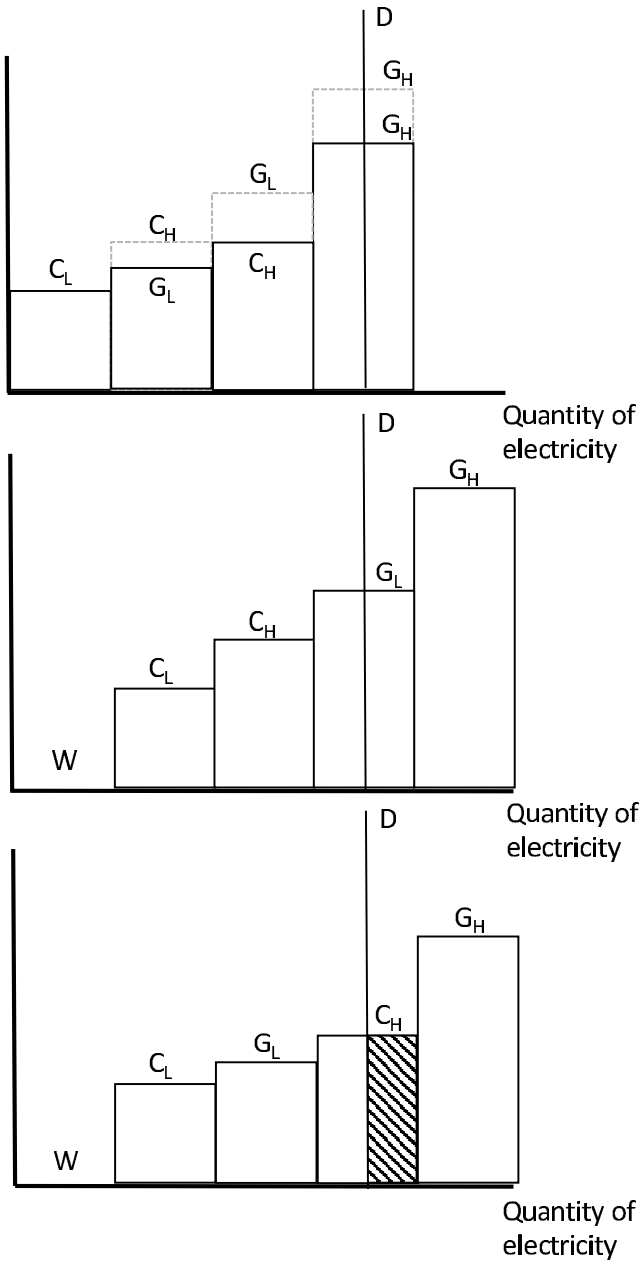

Figure 3: Dispatch curve example. Panel A illustrates the effect of falling natural gas price in isolation. Panel B illustrates the effect of increased wind generation in isolation. Panel C illustrates the joint effect of falling natural gas prices and increased wind generation.

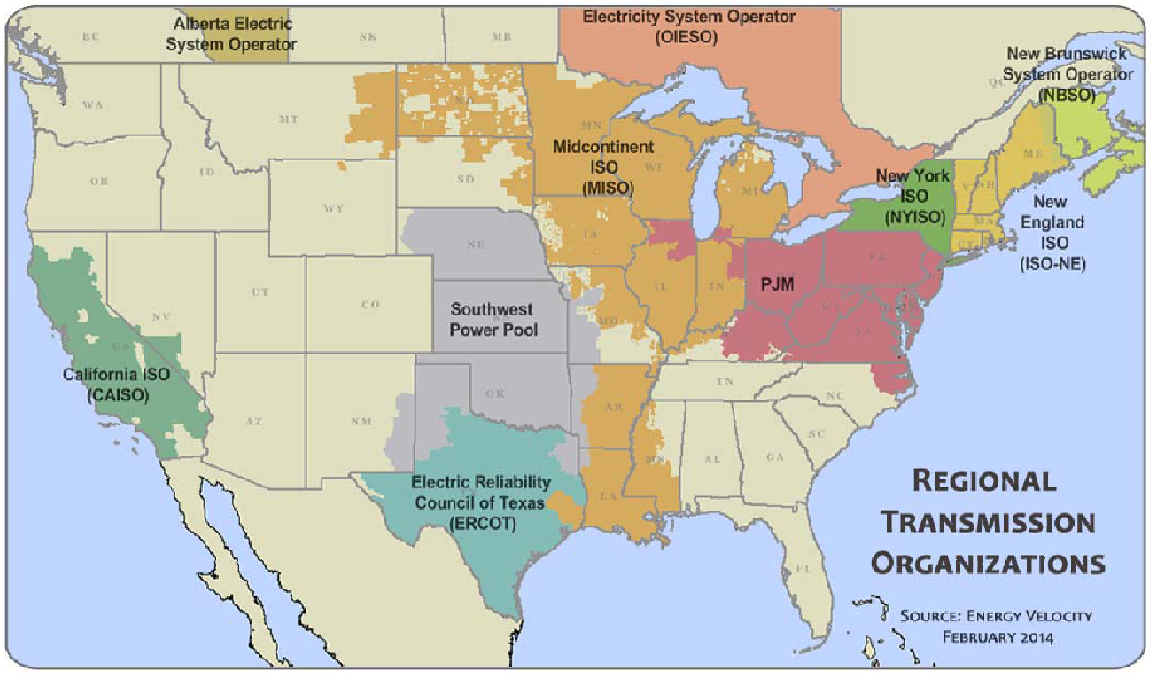

Figure 4: United States ISO/RTO regions. ERCOT, MISO, PJM, and SPP are considered in this study. Source: Federal Energy Regulatory Commission (FERC)

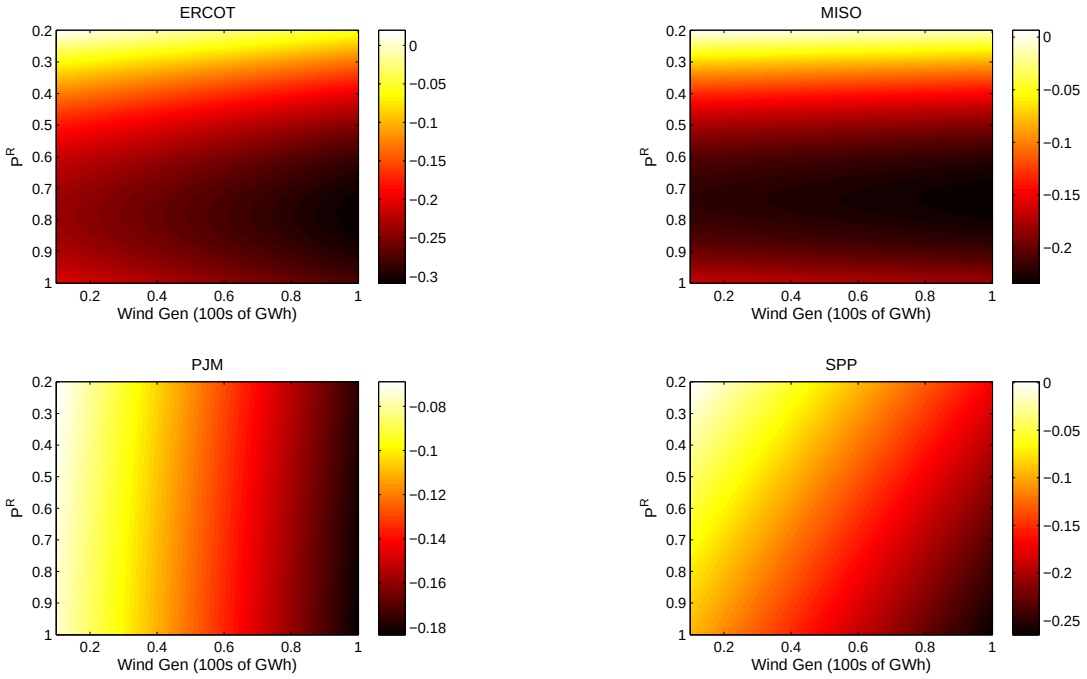

Figure 5: Median Quantile Marginal Effects - $\frac{\partial CF}{\partial P^R}$

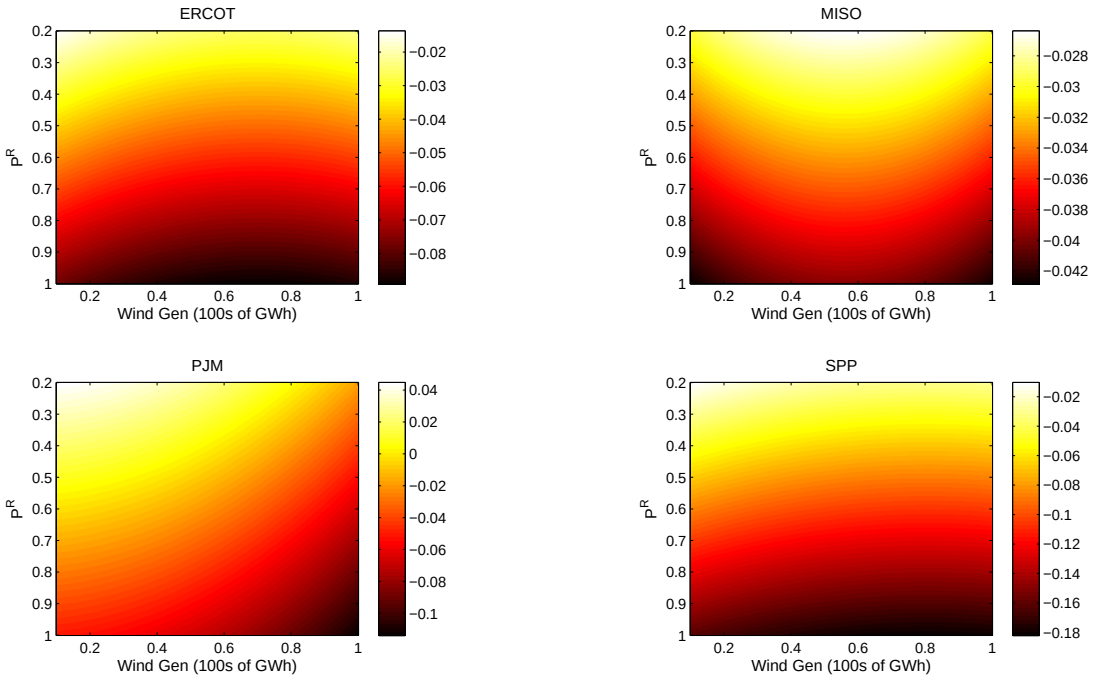

Figure 6: Median Quantile Marginal Effects - $\frac{\partial CF}{\partial W}$

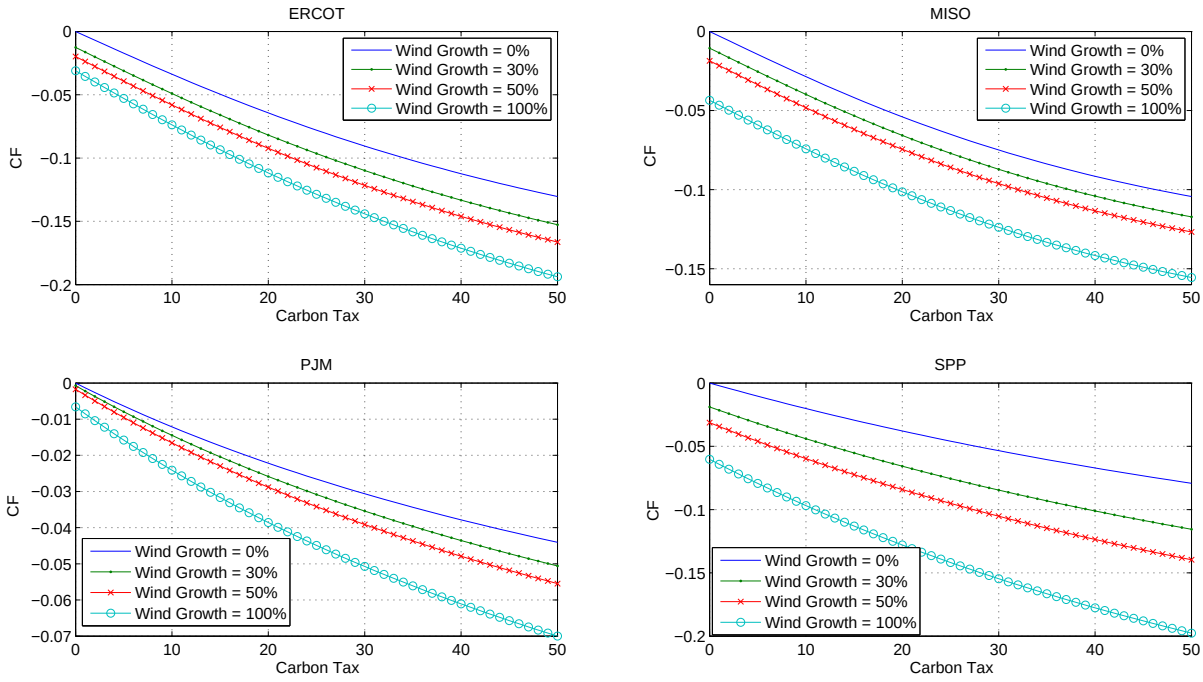

Figure 7: Capacity Factor Response to Emissions Tax

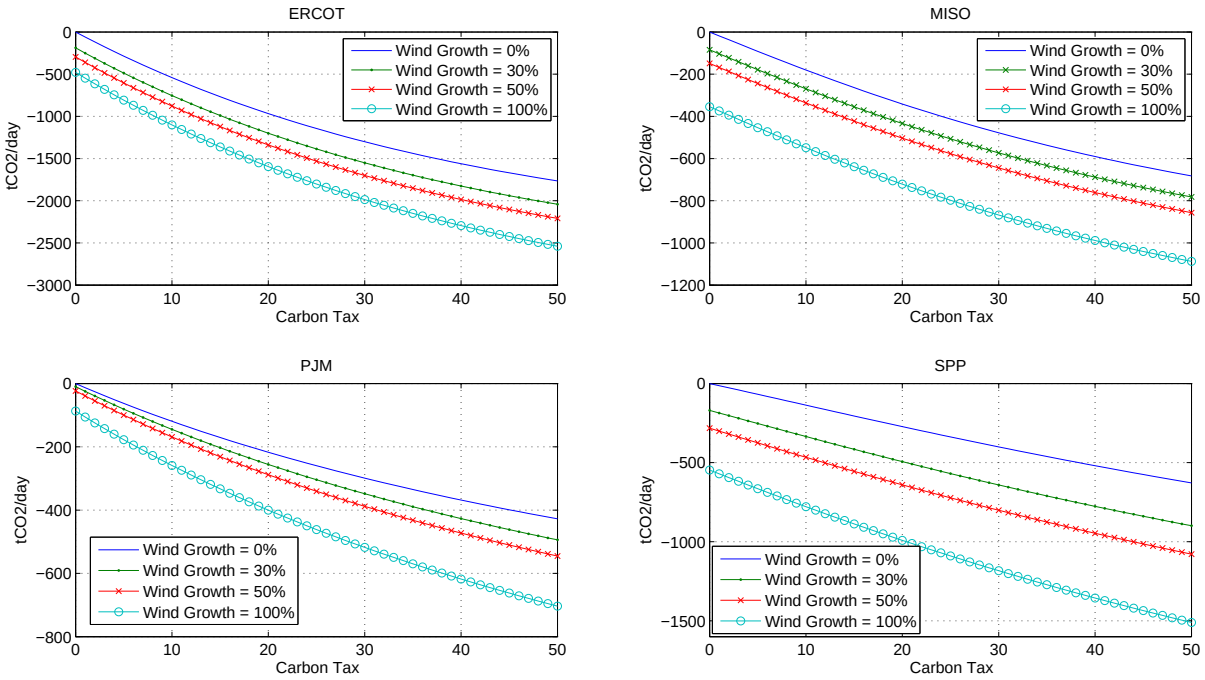

Figure 8: Emissions Response to Emissions Tax

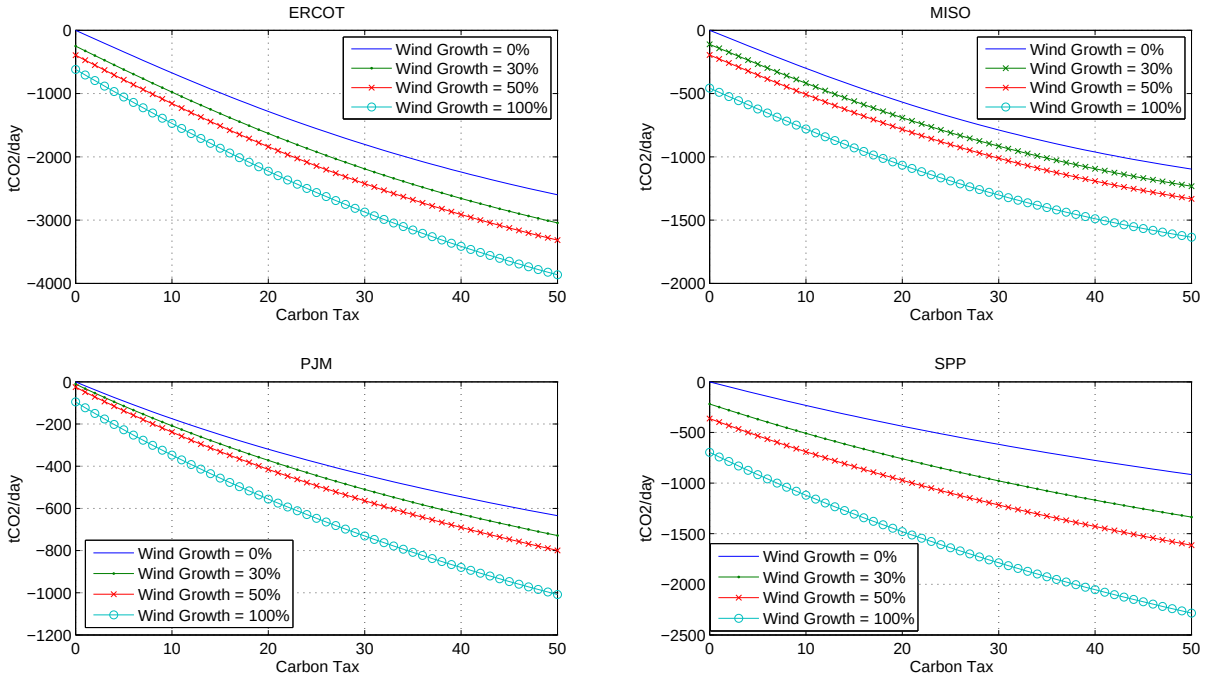

Figure 9: Emissions Response to Emissions Tax - Imputed from CF Reductions